Supplementary Data

Enhanced Magnetic and Optical Properties of $Y_3Fe_5O_{12}$ (YIG) Films with Au Nanoinclusions

Lizabeth Quigley,[1] Katrina Evancho,[1] Claire A. Mihalko,[1] Yizhi Zhang,[1] Chang Liu,[1] Max Chhabra,[1] Bharat Giri,[2] Jialong Huang,[1] Abhijeet Choudhury,[1] Jeremy Gan,[1] Zhengliang Lin,[3] Xiaoshan Xu,[2, 4] Ping Lu,[4] Raktim Sarma,[5, 6] Aleem Siddiqui,[5] Haiyan Wang[1, 3 *]

[1] School of Materials Engineering, Purdue University, West Lafayette, Indiana 47907, USA

[2] Department of Physics and Astronomy, University of Nebraska-Lincoln, Lincoln, Nebraska 68588, USA

[3] School of Electrical and Computer Engineering, Purdue University, West Lafayette, Indiana 47907, USA

[4] Nebraska Center of Materials and Nanoscience, University of Nebraska-Lincoln, Lincoln, Nebraska 68588, USA

[5] Sandia National Laboratory, Albuquerque, New Mexico 87185, USA

[6] Center for Integrated Nanotechnologies, Sandia National Laboratory, Albuquerque, New Mexico 87175, USA

*Corresponding Author: hwang00@purdue.edu

The Supporting Information contains the following Figures and Tables:

Table S1: List of Deposition and Where the Data can be Found

Figure S1: The near zero region for: A1) Real permittivity and A2) Imaginary permittivity of the Pure YIG, Annealed and Thin Au Strip, As Deposited samples. B1) Real permittivity and B2) Imaginary permittivity of the Thin Au Strip, Annealed and Thick Au Strip, As Deposited samples.

Figure S2: XRD θ-2θ for the following Annealed samples on GGG substrates: A) Pure YIG, B) Thin Au Strip, C) Thick Au Strip, D) Au Buffer.

Figure S3: XRD θ-2θ for the following As Deposited samples on GGG substrates: A) Pure YIG, B) Thin Au Strip, C) Thick Au Strip, D) Au Buffer.

Figure S4: A1) Real permittivity and A2) Imaginary permittivity of the Annealed samples on GGG substrates. B1) Real permittivity and B2) Imaginary permittivity of As Deposited samples on GGG substrates.

Figure S5: The nero zero region for: A1) Real permittivity and A2) Imaginary permittivity of the Annealed samples on GGG substrates. B1) Real permittivity and B2) Imaginary permittivity of As Deposited samples on GGG substrates.

Table S2: List of GGG substrate samples hyperbolic ranges and hyperbolic types.

Figure S6: A) Transmittance data for the Annealed samples on GGG substrates. B) Transmittance data for the As Deposited samples on GGG substrates. Both have plasmonic resonances marked as needed.

Figure S7: Magnetic hysteresis data for the Annealed samples on GGG substrates at A1) 300 K and A2) 10 K. For the As Deposited samples on GGG substrates at B1) 300 K and B2) 10 K.

Figure S8: All measured frequencies for the Annealed samples on GGG substrates, specifically: A1) Pure YIG B1) Thin Au Strip C1) Thick Au Strip D1) Au Buffer samples. Selected frequency for the Annealed samples on GGG substrates, specifically: A2) Pure YIG B2) Thin Au Strip C2) Thick Au Strip D2) Au Buffer samples. E1) Graph showing the width of the frequency peaks versus the frequency they appear at for all four shown samples. E2) Graph showing the frequency resonance peaks appear at versus where the peaks occur for all four shown samples.

Figure S9: All measured frequencies for the As Deposited samples on GGG substrates, specifically: A1) Pure YIG B1) Thin Au Strip C1) Thick Au Strip D1) Au Buffer samples. Selected frequency for the As Deposited samples on GGG substrates, specifically: A2) Pure YIG B2) Thin Au Strip C2) Thick Au Strip D2) Au Buffer samples. E1) Graph showing the width of the frequency peaks versus the frequency they appear at for all four shown samples. E2) Graph showing the frequency resonance peaks appear at versus where the peaks occur for all four shown samples.

Table S3: List of the Gilbert damping coefficient, dH0, Gyromagnetic ratio, and Meff for the samples on GGG substrates.

Figure S10: Graph Demonstrating Relative Amount of Au in the Films versus the Measured Gilbert Damping Coefficient (α)

Figure S11: On GGG substrates: A) Annealed Pure YIG, B) As-Deposited Thin Au Strip, C) Annealed Thick Au Strip, D) Annealed Au Buffer. 1) Ideal schematic drawing of the sample, 2) TEM image of the sample 3) STEM image for the corresponding EDS map of the sample, 4) EDS map of the sample.

Table S4: Sample Thickness of Films grown on GGG Substrates

Figure S12: On GGG substrates: A) P-MOKE for the Annealed Thin Au Strip sample, B) P-MOKE for the As-Deposited Thin Au Strip sample, C) L-MOKE for the Annealed Thin Au Strip sample, D) L-MOKE for the As-Deposited Thin Au Strip sample, E) A smaller measured region for L-MOKE for the Annealed Thin Au Strip sample, and F) A smaller measured region for the L-MOKE for the As-Deposited Thin Au Strip sample.

Figure S13: XRD θ-2θ for the following Annealed samples on STO substrates: A) Pure YIG, B) Thin Au Strip, C) Thick Au Strip, D) Au Buffer.

Figure S14: XRD θ-2θ for the following As Deposited samples on STO substrates: A) Pure YIG, B) Thin Au Strip, C) Thick Au Strip, D) Au Buffer.

Figure S15: A1) Real permittivity and A2) Imaginary permittivity of the Annealed samples on STO substrates. B1) Real permittivity and B2) Imaginary permittivity of As Deposited samples on STO substrates.

Figure S16: The near zero region for: A1) Real permittivity and A2) Imaginary permittivity of the Annealed samples on STO substrates. B1) Real permittivity and B2) Imaginary permittivity of As Deposited samples on STO substrates.

Table S5: List of STO substrate samples hyperbolic ranges and hyperbolic types.

Figure S17: A) Transmittance data for the Annealed samples on STO substrates. B) Transmittance data for the As Deposited samples on STO substrates. Both have plasmonic resonances marked as needed.

Figure S18: Magnetic hysteresis data for the Annealed samples on STO substrates at A1) 300 K and A2) 10 K. For the As Deposited samples on STO substrates at B1) 300 K and B2) 10 K.

Table S6: List of the Saturation Magnetization and Coercivity for all the samples grown on STO substrates.

Figure S19: All measured frequencies for the Annealed samples on STO substrates, specifically: A1) Pure YIG B1) Thin Au Strip C1) Thick Au Strip D1) Au Buffer samples. Selected frequency for the Annealed samples on GGG substrates, specifically: A2) Pure YIG B2) Thin Au Strip C2) Thick Au Strip D2) Au Buffer samples. E1) Graph showing the width of the frequency peaks versus the frequency they appear at for all four shown samples. E2) Graph showing the frequency resonance peaks appear at versus where the peaks occur for all four shown samples.

Figure S20: All measured frequencies for the As Deposited samples on STO substrates, specifically: A1) Pure YIG B1) Thin Au Strip C1) Thick Au Strip D1) Au Buffer samples. Selected frequency for the As Deposited samples on GGG substrates, specifically: A2) Pure YIG B2) Thin Au Strip C2) Thick Au Strip D2) Au Buffer samples. E1) Graph showing the width of the frequency peaks versus the frequency they appear at for all four shown samples. E2) Graph showing the frequency resonance peaks appear at versus where the peaks occur for all four shown samples.

Figure S21: On STO substrates: A) Annealed Pure YIG, B) As-Deposited Pure YIG, C) Annealed Thin Au Strip, D) As-Deposited Thin Au Strip, E) Annealed Thick Au Strip, F) As-Deposited Au Strip, G) Annealed Au Buffer, H) As-Deposited Au Buffer. 1) Ideal schematic drawing of the sample, 2) TEM image of the sample 3) STEM image for the corresponding EDS map of the sample, 4) EDS map of the sample.

Table S7: Sample Thickness of Films grown on STO Substrates

Table S1: List of Deposition and Where the Data can be Found

Type of Deposition	Annealing?	Substrate?	Data in the main text?
Pure YIG	Yes	GGG	Yes
		STO	Only TEM
	No	GGG	Supplementary Only
		STO	
Thin Au Strip	Yes	GGG	Yes
		STO	Only TEM
	No	GGG	Yes
		STO	Only TEM
Thick Au Strip	Yes	GGG	Supplementary Only
		STO	
	No	GGG	Yes
		STO	Only TEM
Au Buffer Layer*	Yes	GGG	Supplementary Only
		STO	
	No	GGG	
		STO	

*The Au Buffer Layer sample has the buffer layer composition of YIG-Au followed by a deposition of pure YIG, as described in the Experimental Methods section of the manuscript.

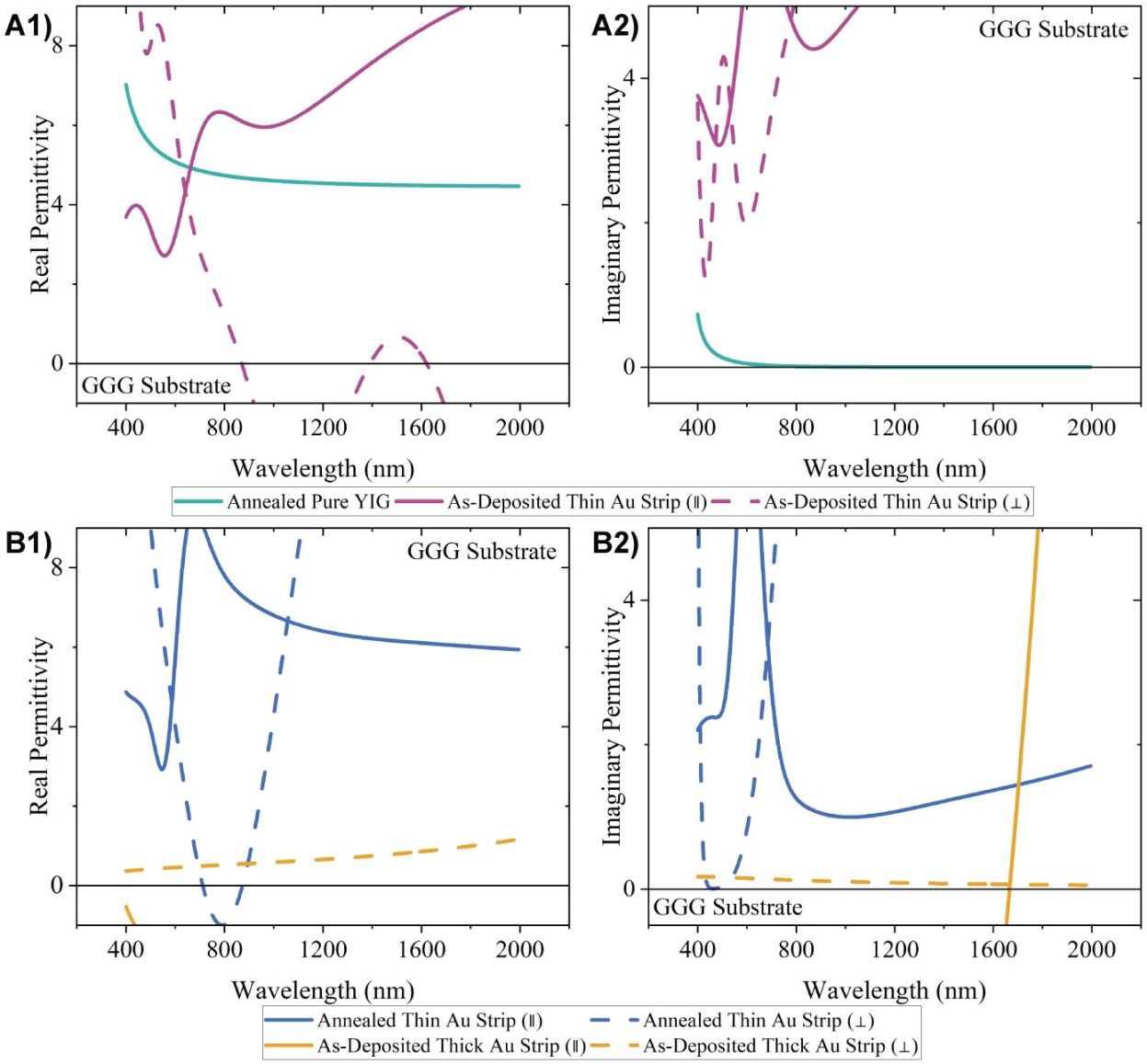

Figure S1: The near zero region for: A1) Real permittivity and A2) Imaginary permittivity of the Annealed Pure YIG and As-Deposited Thin Au Strip samples. B1) Real permittivity and B2) Imaginary permittivity of the Annealed with Thin Au Strip and As-Deposited with Thick Au Strip samples.

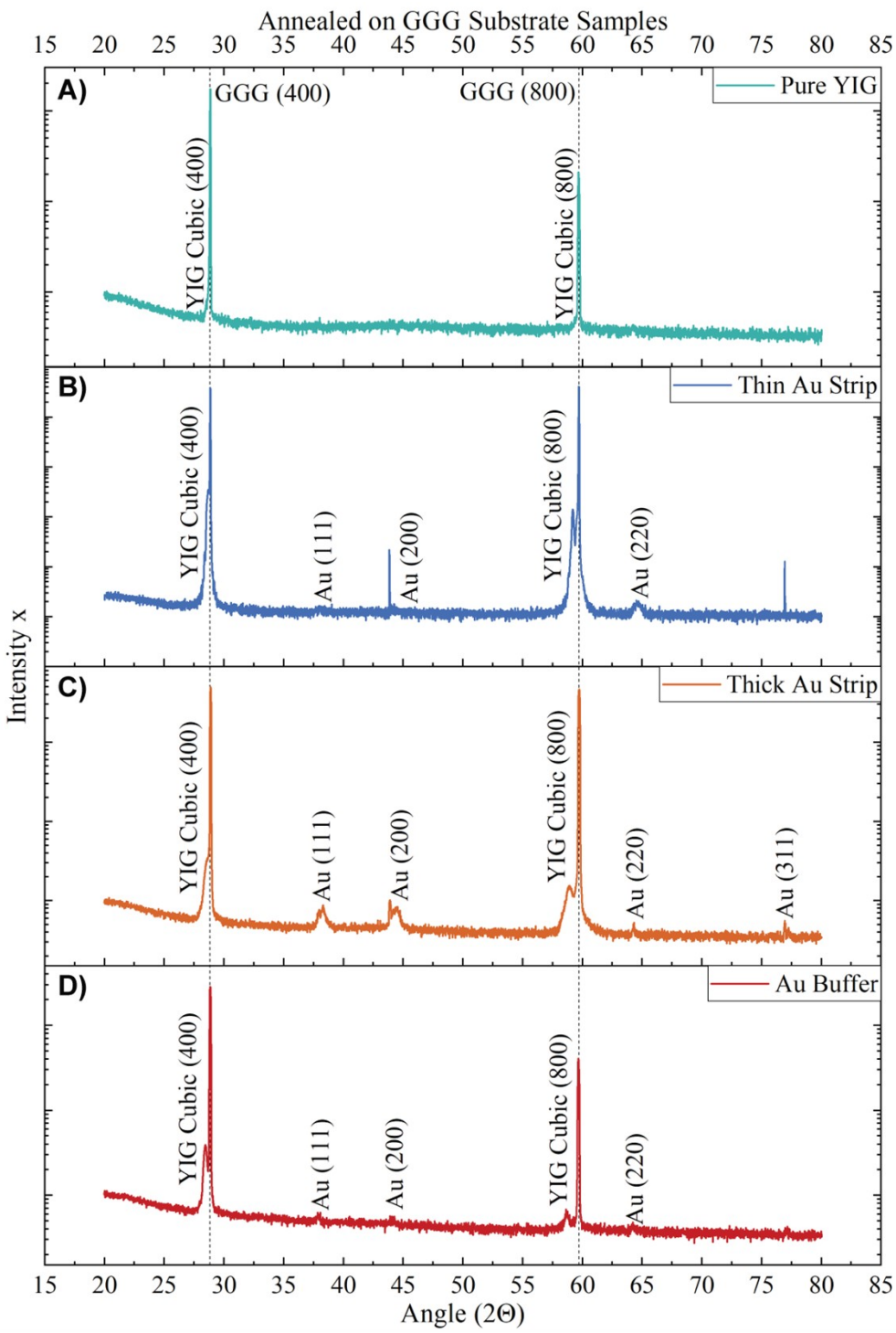

Figure S2: XRD θ-2θ for the following Annealed samples on GGG substrates: A) Pure YIG, B) Thin Au Strip, C) Thick Au Strip, D) Au Buffer.

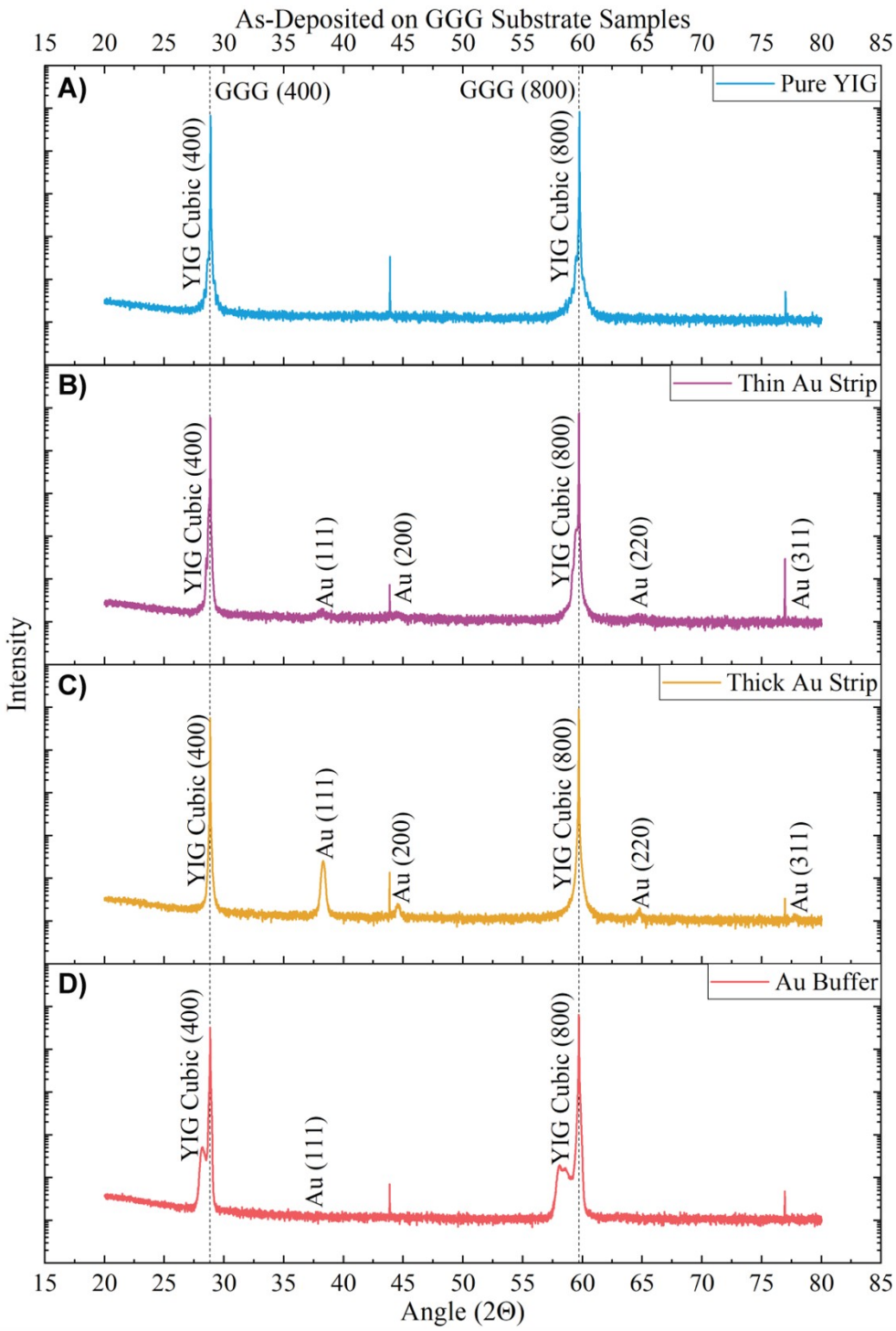

Figure S3: XRD θ-2θ for the following As-Deposited samples on GGG substrates: A) Pure YIG, B) Thin Au Strip, C) Thick Au Strip, D) Au Buffer.

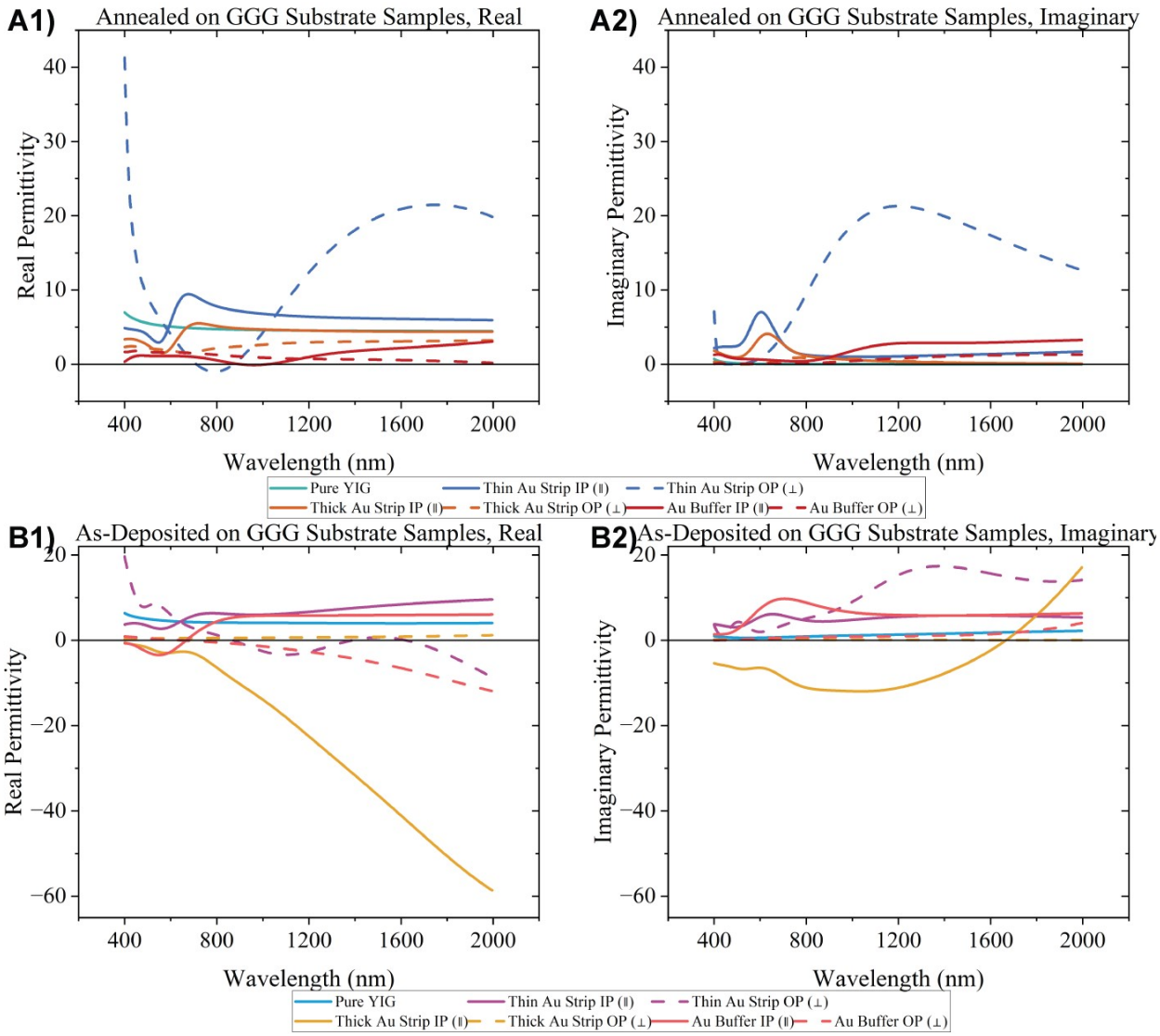

Figure S4: A1) Real permittivity and A2) Imaginary permittivity of the Annealed samples on GGG substrates. B1) Real permittivity and B2) Imaginary permittivity of As-Deposited samples on GGG substrates.

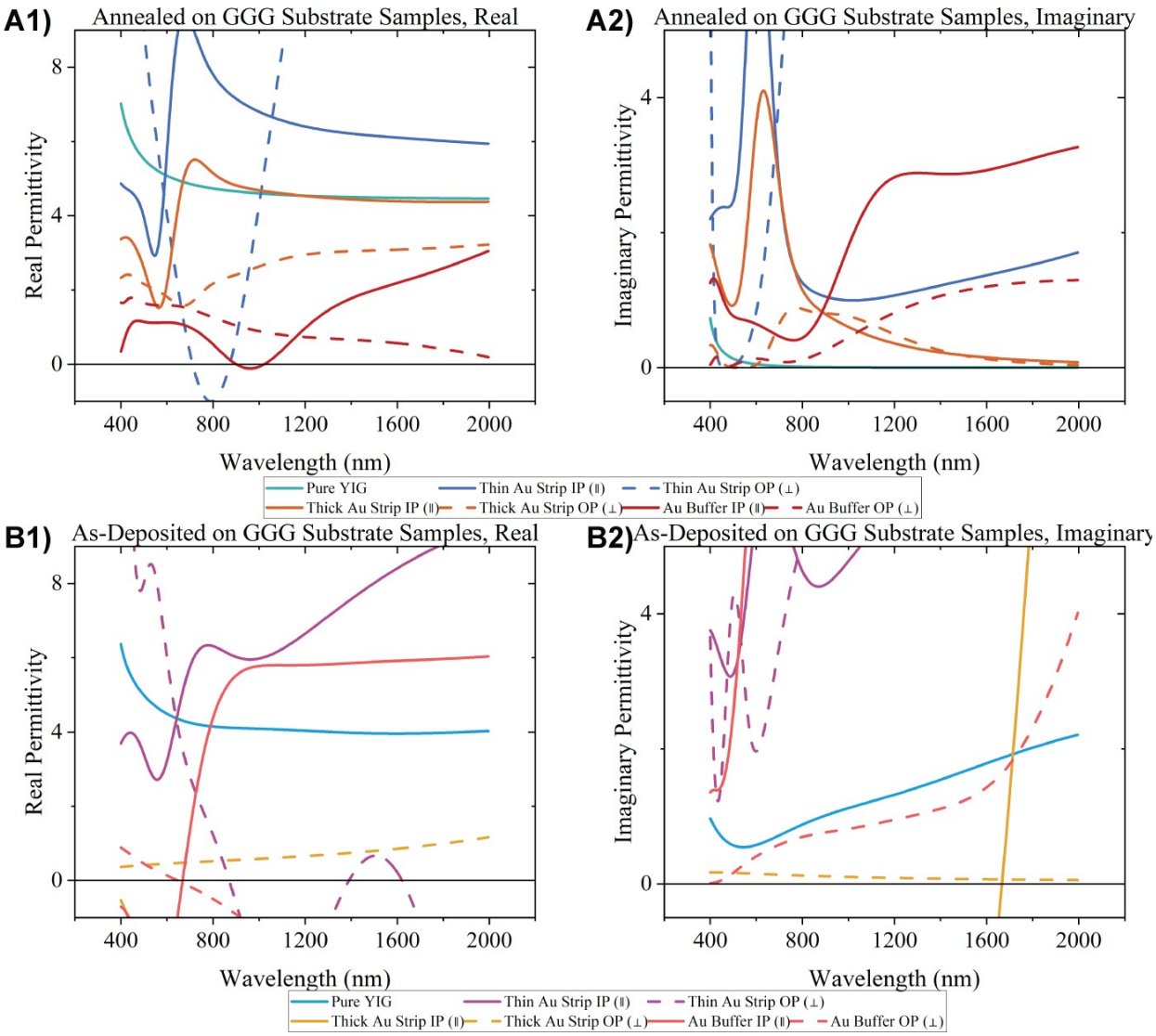

Figure S5: The near zero region for: A1) Real permittivity and A2) Imaginary permittivity of the Annealed samples on GGG substrates. B1) Real permittivity and B2) Imaginary permittivity of As-Deposited samples on GGG substrates.

Table S2: List of GGG substrate samples hyperbolic ranges and hyperbolic types.

	Hyperbolic Type	Hyperbolic Range (nm)
Annealed Pure YIG	N/A	
Annealed Thin Au Strip	Type-I	712-873
Annealed Thick Au Strip	N/A	
Annealed Au Buffer	Type-I	902-1018
As-Deposited Pure YIG	N/A	
As-Deposited Thin Au Strip	Type-I	871-1390
		1624-2000
As-Deposited Thick Au Strip	Type-II	400-2000
As-Deposited Au Buffer	Type-II	400-646
	Type-I	669-2000

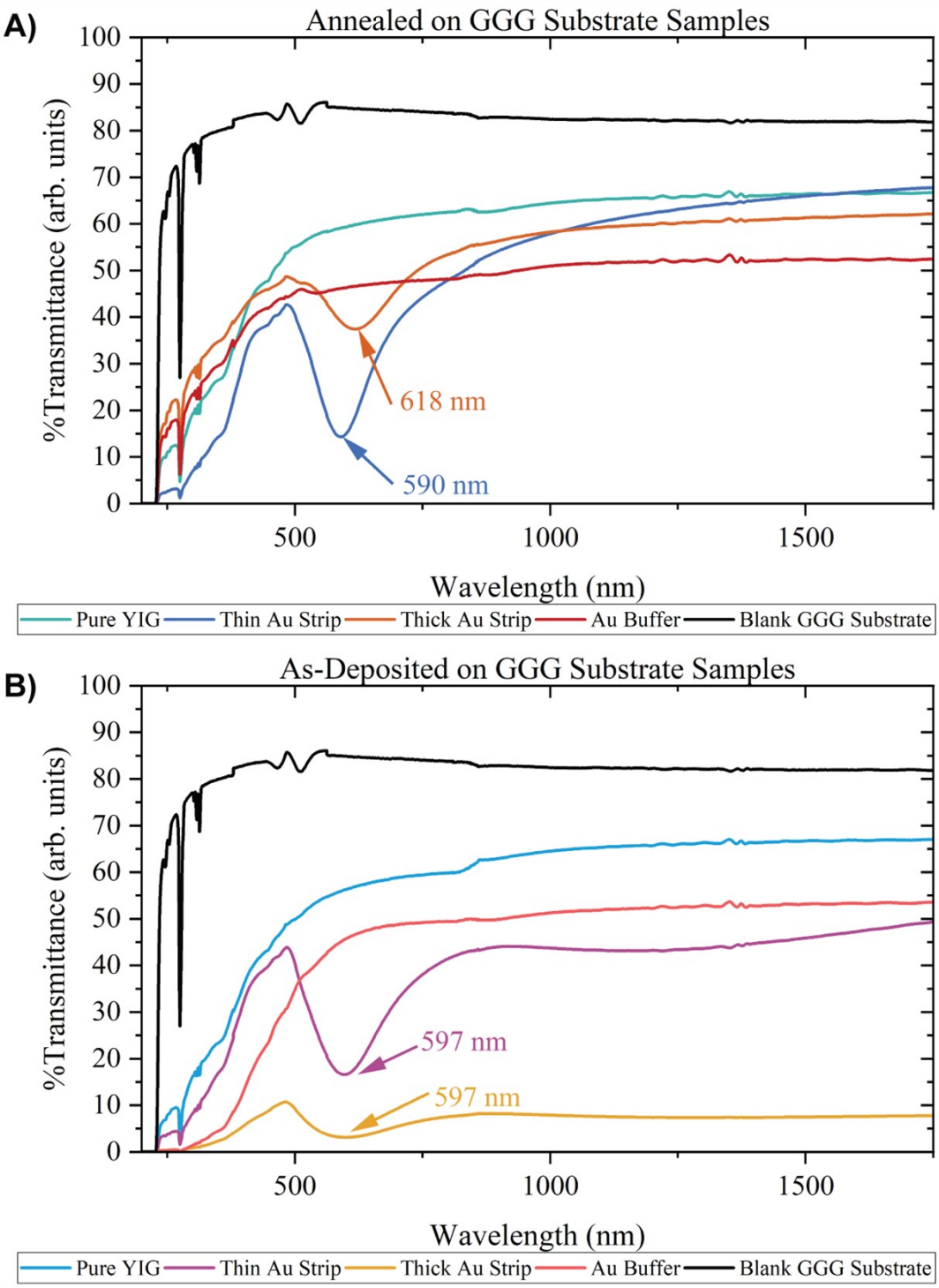

Figure S6: A) Transmittance data for the Annealed samples on GGG substrates. B) Transmittance data for the As-Deposited samples on GGG substrates. Both have plasmonic resonances marked as needed.

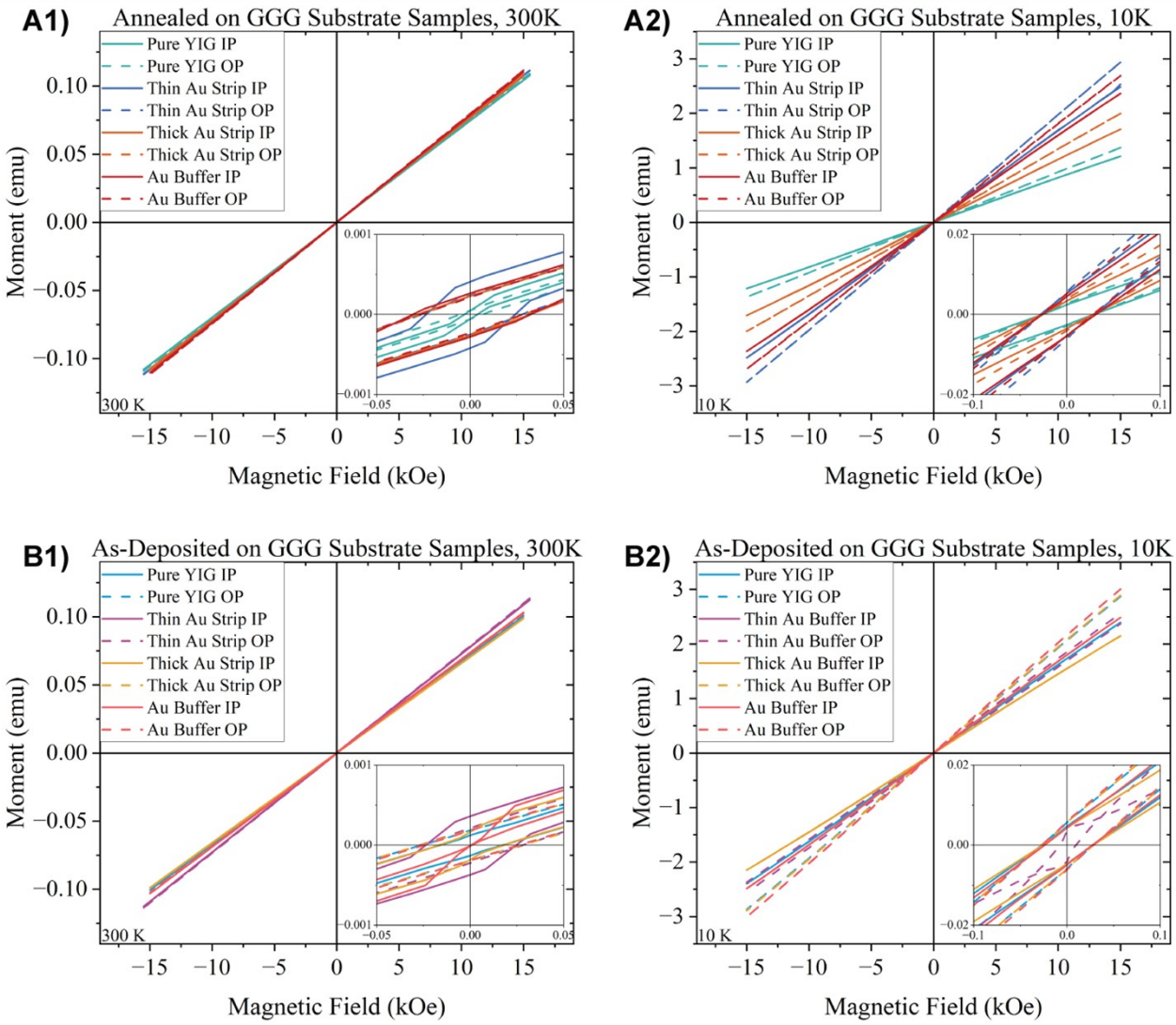

Figure S7: Magnetic hysteresis data for the Annealed samples on GGG substrates at A1) 300 K and A2) 10 K. For the As-Deposited samples on GGG substrates at B1) 300 K and B2) 10 K.

GGG, the substrate, is known for being paramagnetic. We attempted to subtract out its effect on the film, but to no success. The insets in Figure S7 does allow for slight differences between each film to be seen, which is why this data is still reported. However, because the effects of GGG substrate could not be removed from the data, the film's saturation and coercivity is not reported here in a table. The companion STO samples, as seen in Figure S18, do have proper hysteresis loops, and are assumed to be representative of these films.

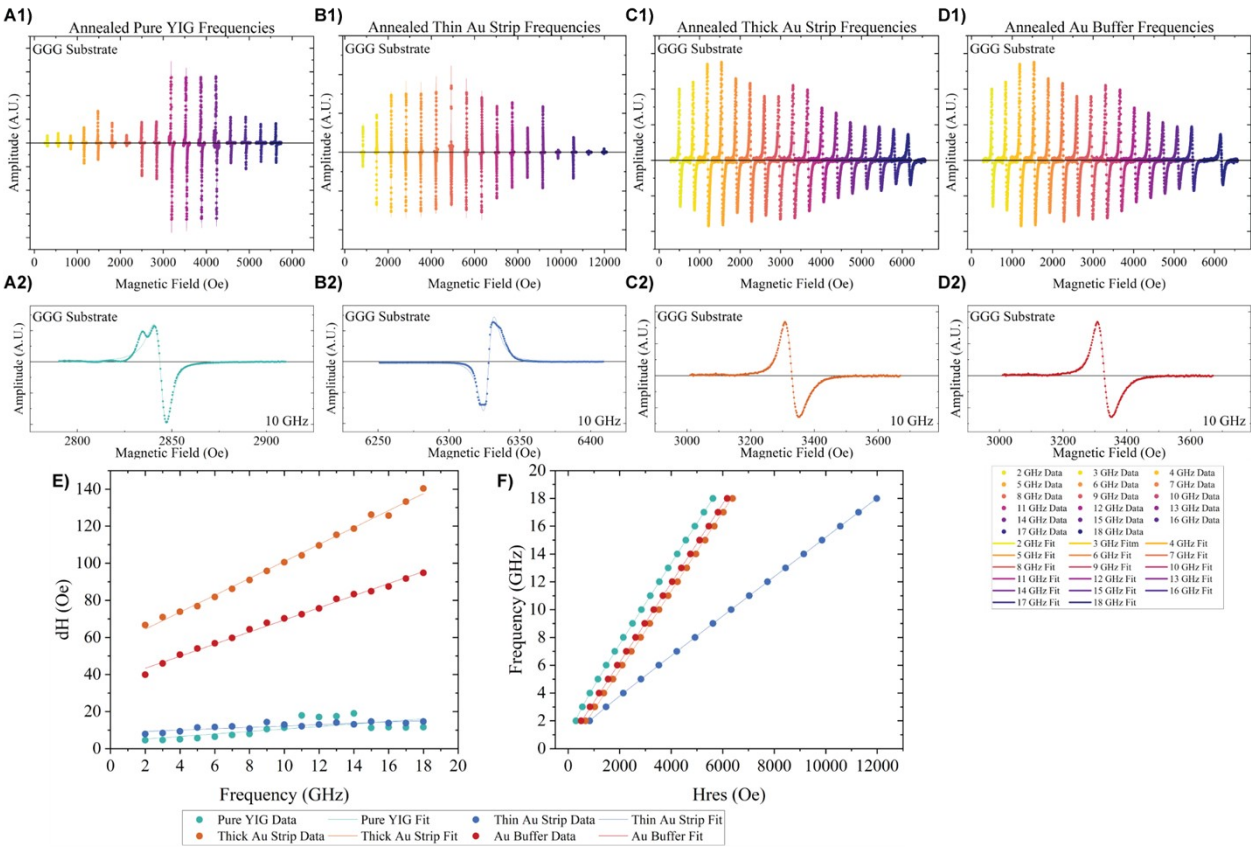

Figure S8: Ferromagnetic resonance measurement results of the Annealed samples on GGG substrates A) Pure YIG, B) Thin Au Strip, C) Thick Au Strip, D) Au Buffer. 1) All measured frequencies. 2) Selected 10 GHz frequency. E) Graph showing the width of the frequency peaks versus the frequency they appear at for all four shown samples. F) Graph showing the frequency resonance peaks appear at versus where the peaks occur for all four shown samples.

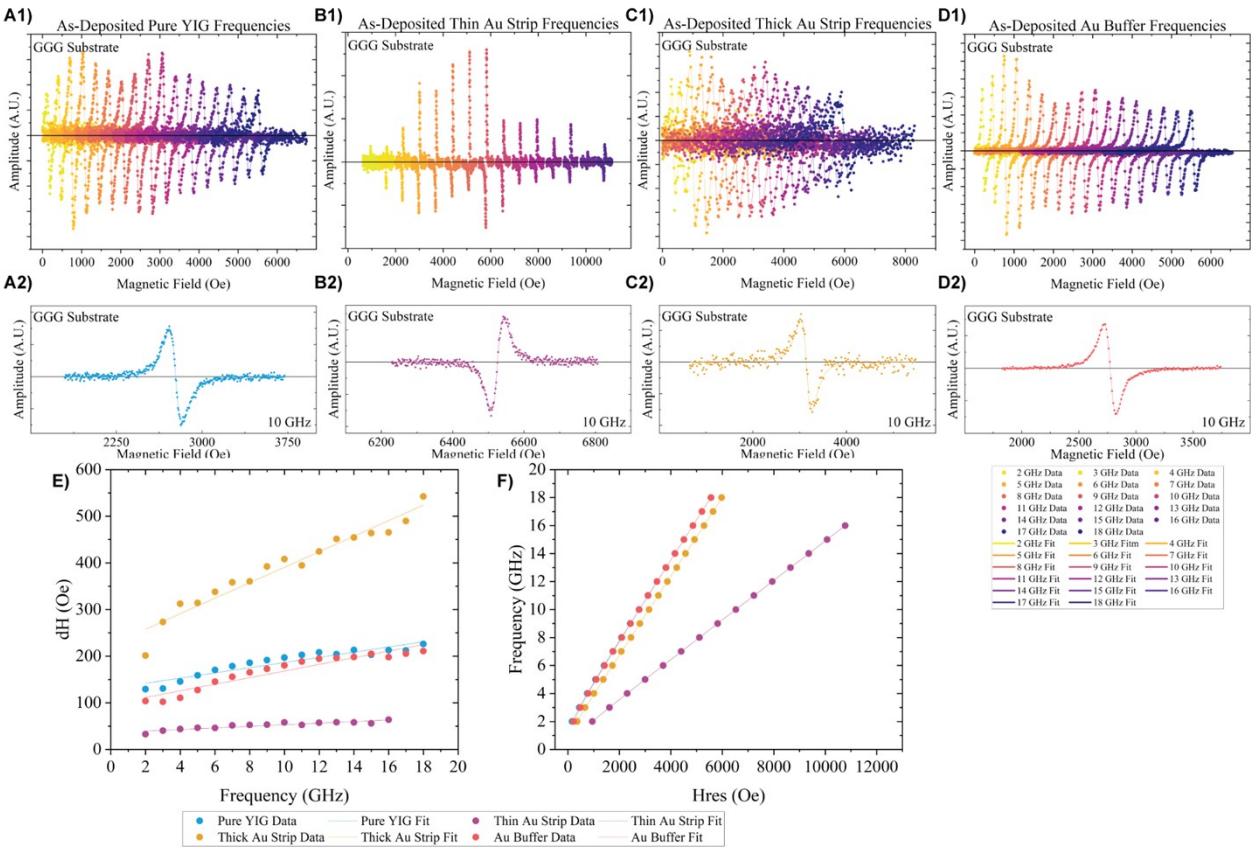

Figure S9: Ferromagnetic resonance measurement results of the As-Deposited samples on GGG substrates A) Pure YIG, B) Thin Au Strip, C) Thick Au Strip, D) Au Buffer. 1) All measured frequencies. 2) Selected 10 GHz frequency. E) Graph showing the width of the frequency peaks versus the frequency they appear at for all four shown samples. F) Graph showing the frequency resonance peaks appear at versus where the peaks occur for all four shown samples.

Table S3: List of the Gilbert damping coefficient, dH_0, Gyromagnetic ratio, and M_{eff} for the samples on GGG substrates.

	Gilbert Damping Coefficient (α)	dH_0 (Oe)	Gyromagnetic Ratio (γ) (GHz/T)	M_{eff} (Oe)
Annealed Pure YIG	9.66×10^{-4}	3.85	28.5	0.148
Annealed Thin Au Strip	2.58×10^{-4}	8.57	14.1	0.161
Annealed Thick Au Strip	6.51×10^{-3}	55.3	28.5	$2x10^{-6}$
Annealed Au Buffer	4.65×10^{-3}	36.8	28.5	$-2x10^{-6}$
As-Deposited Pure YIG	7.91×10^{-3}	130.8	28.4	0.135
As-Deposited Thin Au Strip	1.19×10^{-3}	36.23	14.1	0.120
As-Deposited Thick Au Strip	2.33×10^{-2}	224.6	28.1	0.058
As-Deposited Au Buffer	1.01×10^{-2}	97.28	28.4	0.155

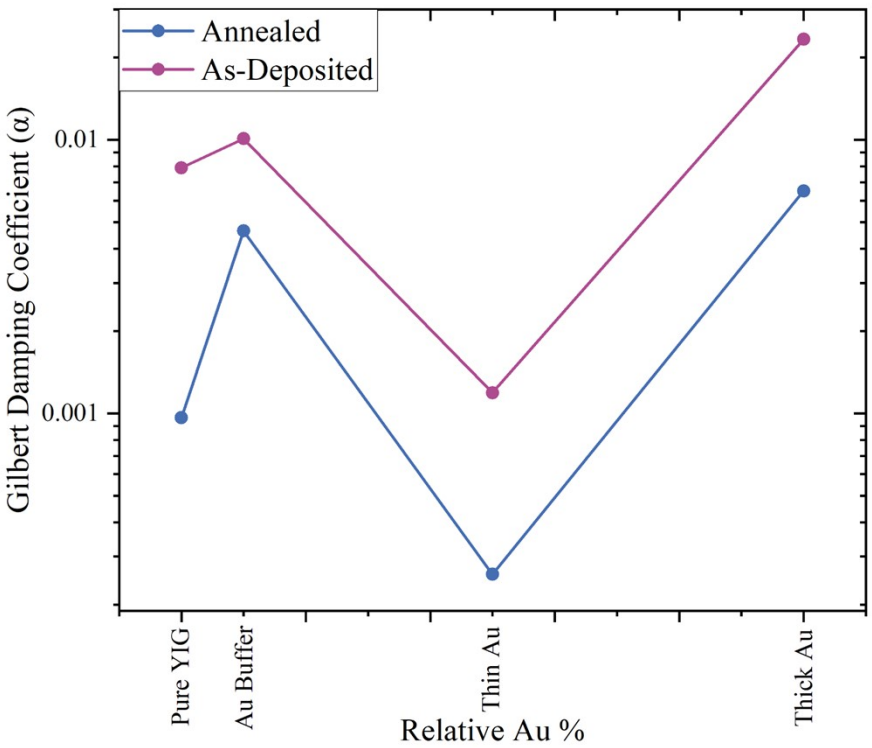

Figure S10: Graph Demonstrating the Measured Gilbert Damping Coefficient (α) based on the different types of Au incorporation.

The fits for these samples show clear trends that are worth a brief discussion. Comparing the two Pure YIG samples supports the claims made in the paper that annealing is necessary to achieve the best magnetic damping. The large difference in dH_0 also suggests that the As Deposited film has more inhomogeneities, strain, or defects within the film, which annealing likely minimizes. This trend continues with all of the annealed vs as-deposited samples. The Thin Au Strip samples have the lowest Gilbert damping both overall, and when you split the samples between annealed and as deposited. This shows that this is an ideal amount of Au that allows for YIG and Au to couple together. The dip in the gyromagnetic ratio is assumed to not be due to measurement error, and because it occurs in both Thin Au Strip samples. Instead, this helps represent the coupling between the YIG-Au interfaces and its beneficial effects on the film, leading to the increased magnetic anisotropy and thus resonance peaks occurring at higher fields than any other measured samples. The Thick Au Samples have the gyromagnetic ratio go back to the normal value, supporting the findings in the main paper that the benefits of the Au nanoinclusions only occur when the Au is at a certain size. The Thick Au Strip samples also have the highest dH_0 out of all the films within the annealed and as deposited categories, showing how the addition of this much Au disrupts the overall crystal structure, leading to the highest magnetic dampings. The two Au Buffer samples were an attempt to have some YIG-Au interfaces which would allow some coupling while having a minimal effect on the microstructure, but instead caused a higher and therefore worse Gilbert damping coefficient, to occur.

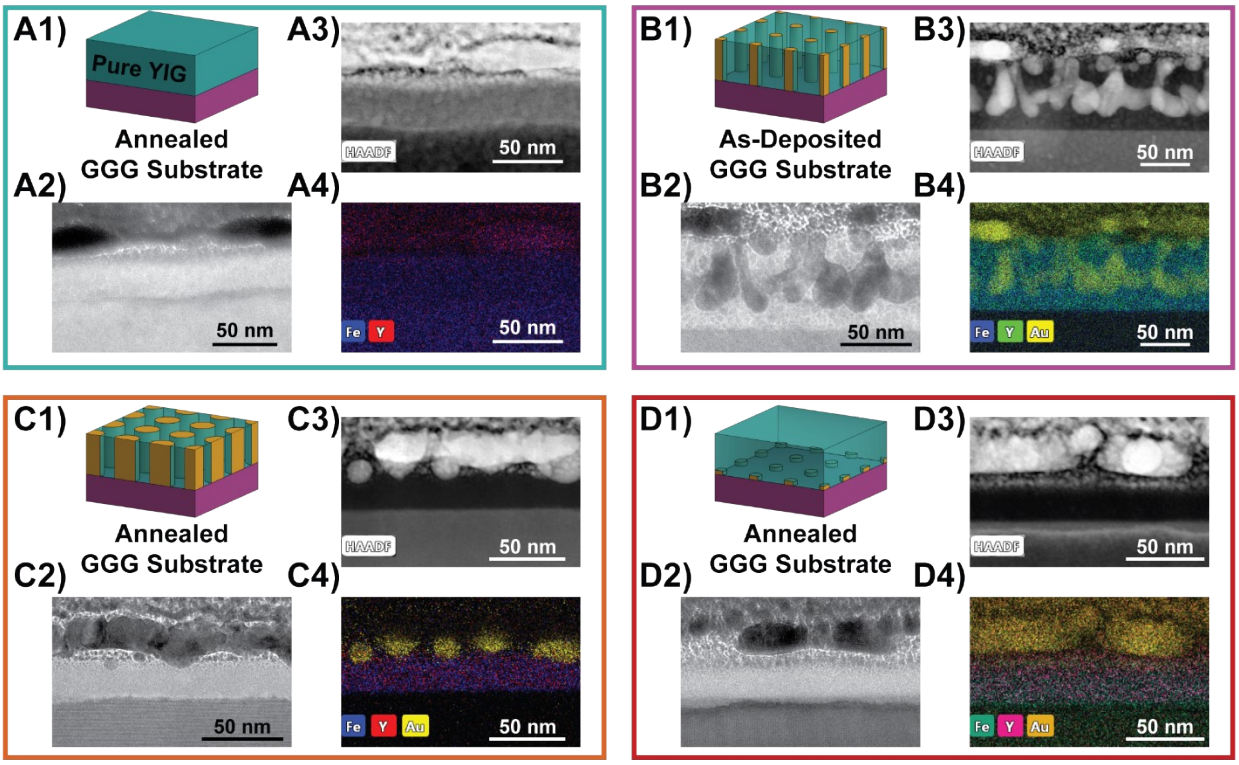

Figure S11: On GGG substrates: A) Annealed Pure YIG, B) As-Deposited Thin Au Strip, C) Annealed Thick Au Strip, D) Annealed Au Buffer. 1) Ideal schematic drawing of the sample, 2) TEM image of the sample 3) STEM image for the corresponding EDS map of the sample, 4) EDS map of the sample.

Table S4: Sample Thickness of Films grown on GGG Substrates

	Film Thickness (nm)
Annealed Pure YIG	38.3
Annealed Thin Au Strip	N/A
Annealed Thick Au Strip	27.5
Annealed Au Buffer	23.3
As-Deposited Pure YIG	N/A
As-Deposited Thin Au Strip	76.8
As-Deposited Thick Au Strip	N/A
As-Deposited Au Buffer	N/A

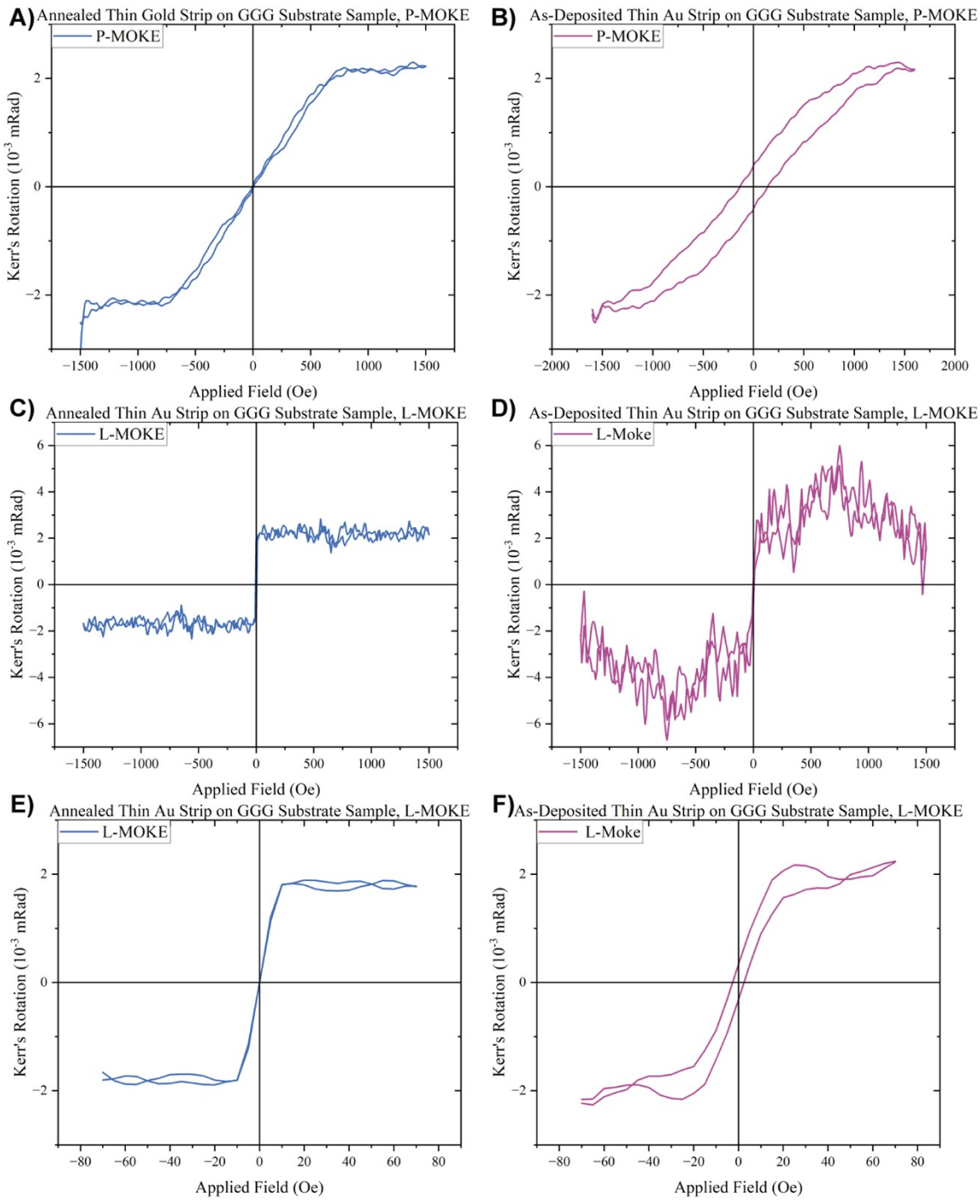

Figure S12: On GGG substrates: A) P-MOKE for the Annealed Thin Au Strip sample, B) P-MOKE for the As-Deposited Thin Au Strip sample, C) L-MOKE for the Annealed Thin Au Strip sample, D) L-MOKE for the As-Deposited Thin Au Strip sample, E) A smaller measured region for L-MOKE for the Annealed Thin Au Strip sample, and F) A smaller measured region for the L-MOKE for the As-Deposited Thin Au Strip sample.

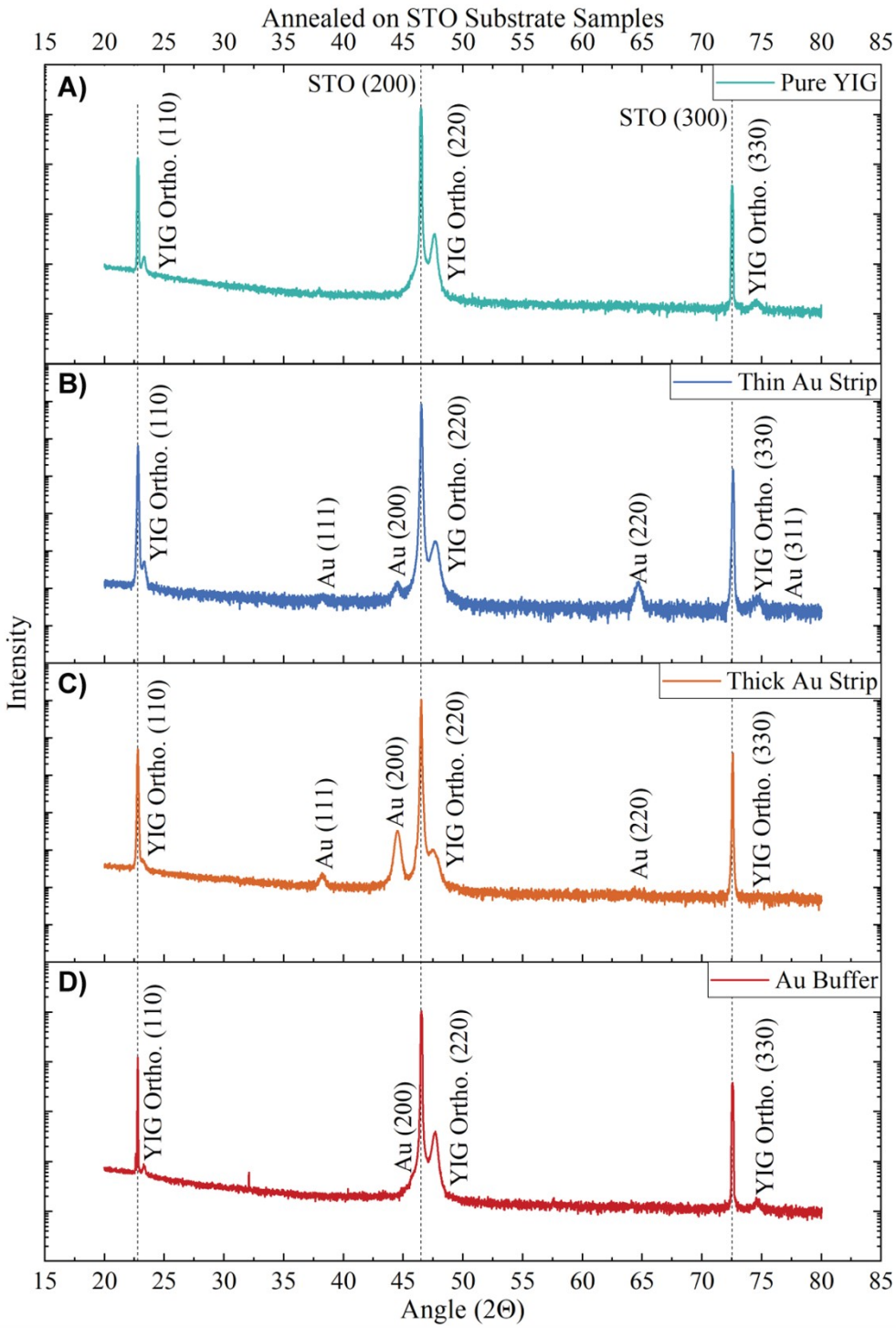

Figure S13: XRD θ-2θ for the following Annealed samples on STO substrates: A) Pure YIG, B) Thin Au Strip, C) Thick Au Strip, D) Au Buffer.

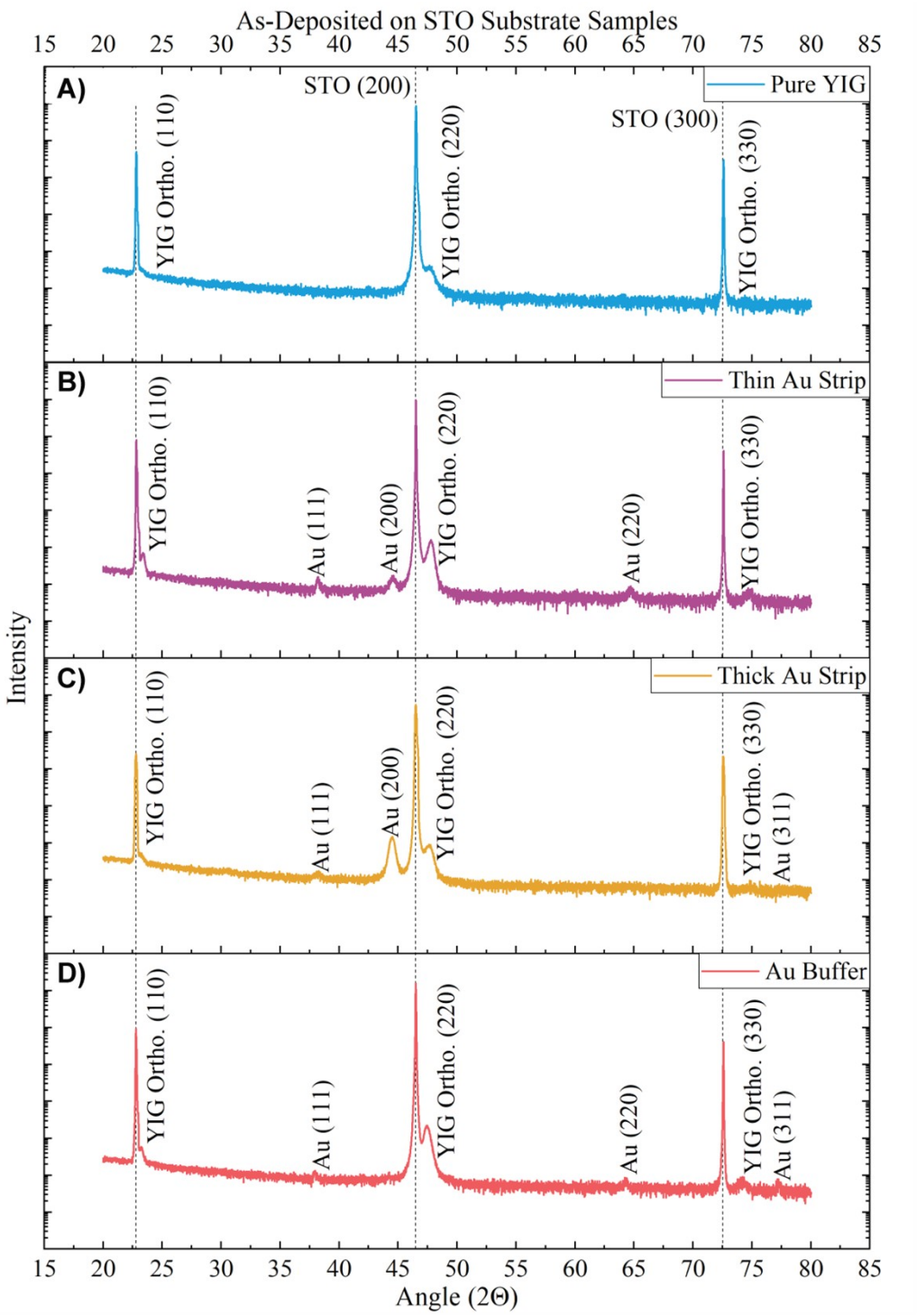

Figure S14: XRD θ-2θ for the following As-Deposited samples on STO substrates: A) Pure YIG, B) Thin Au Strip, C) Thick Au Strip, D) Au Buffer.

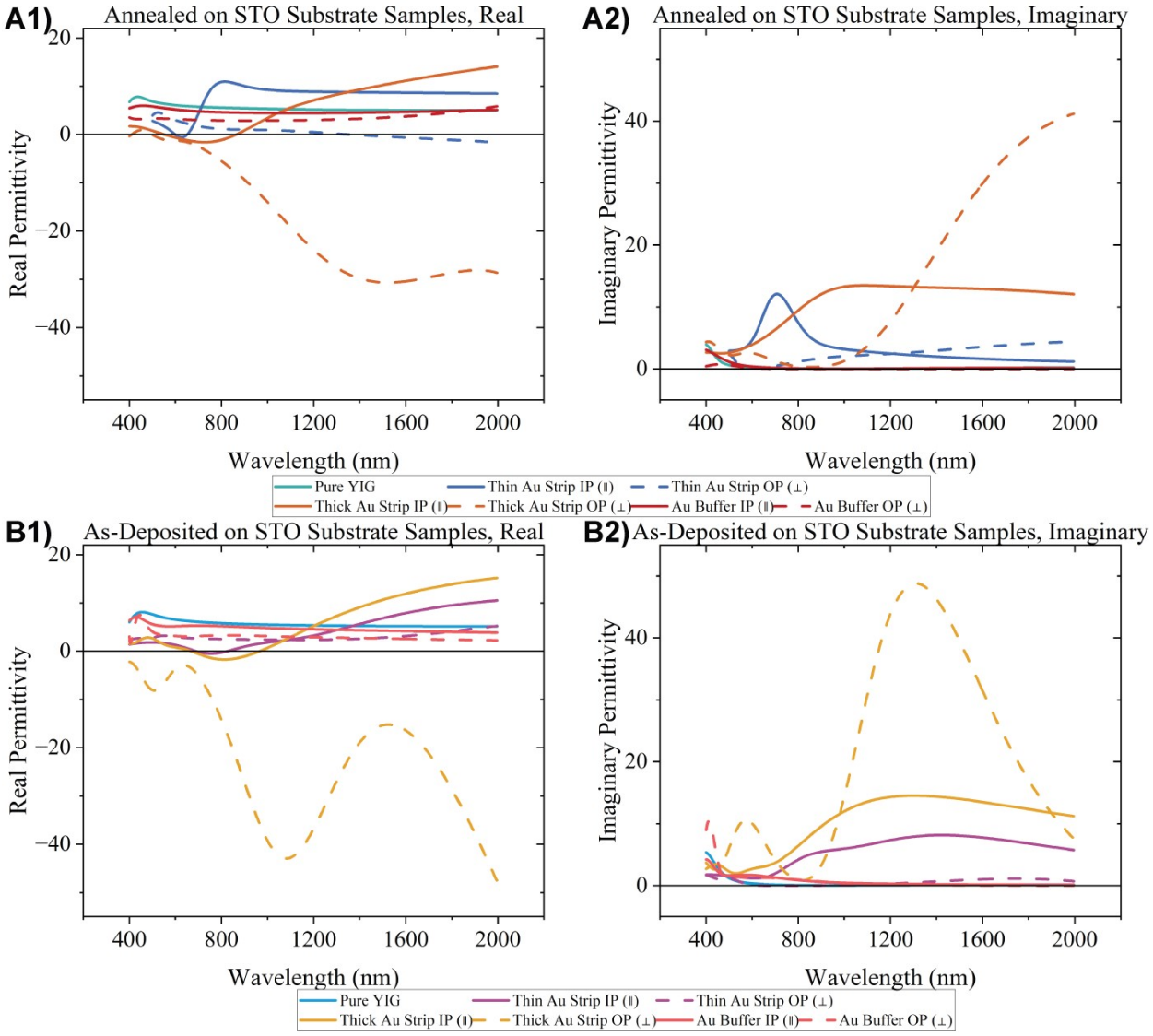

Figure S15: A1) Real permittivity and A2) Imaginary permittivity of the Annealed samples on STO substrates. B1) Real permittivity and B2) Imaginary permittivity of As-Deposited samples on STO substrates.

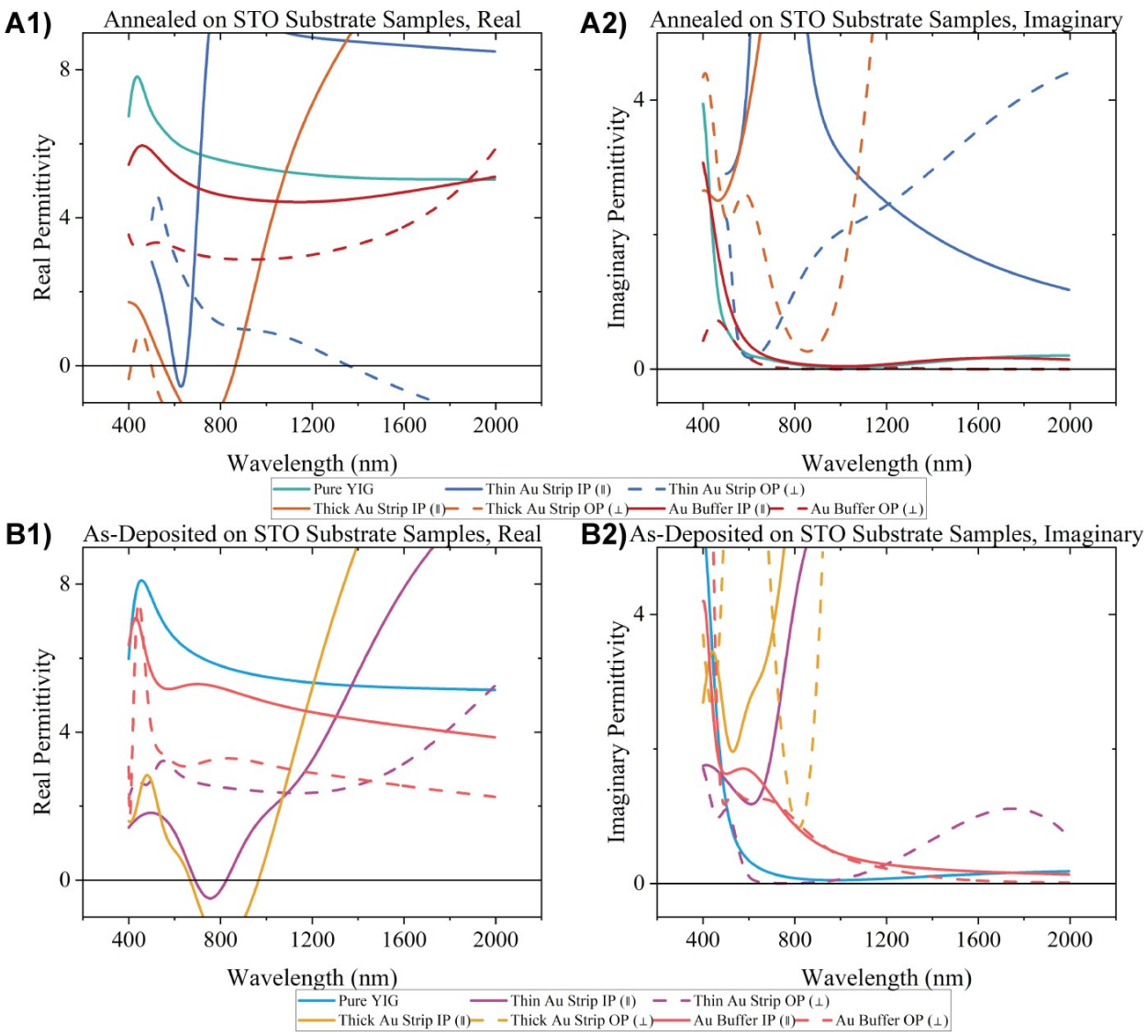

Figure S16: The near zero region for: A1) Real permittivity and A2) Imaginary permittivity of the Annealed samples on STO substrates. B1) Real permittivity and B2) Imaginary permittivity of As-Deposited samples on STO substrates.

Table S5: List of STO substrate samples hyperbolic ranges and hyperbolic types.

	Hyperbolic Type	Hyperbolic Range (nm)
Annealed Pure YIG	N/A	
Annealed Thin Au Strip	Type-II	600-651
	Type-I	1360-2000
Annealed Thick Au Strip	Type-I	400-410
		499-552
		865-2000
Annealed Au Buffer	N/A	
As-Deposited Pure YIG	N/A	
As-Deposited Thin Au Strip	Type-II	690-825
As-Deposited Thick Au Strip	Type-I	300-668
		966-2000
As-Deposited Au Buffer	N/A	

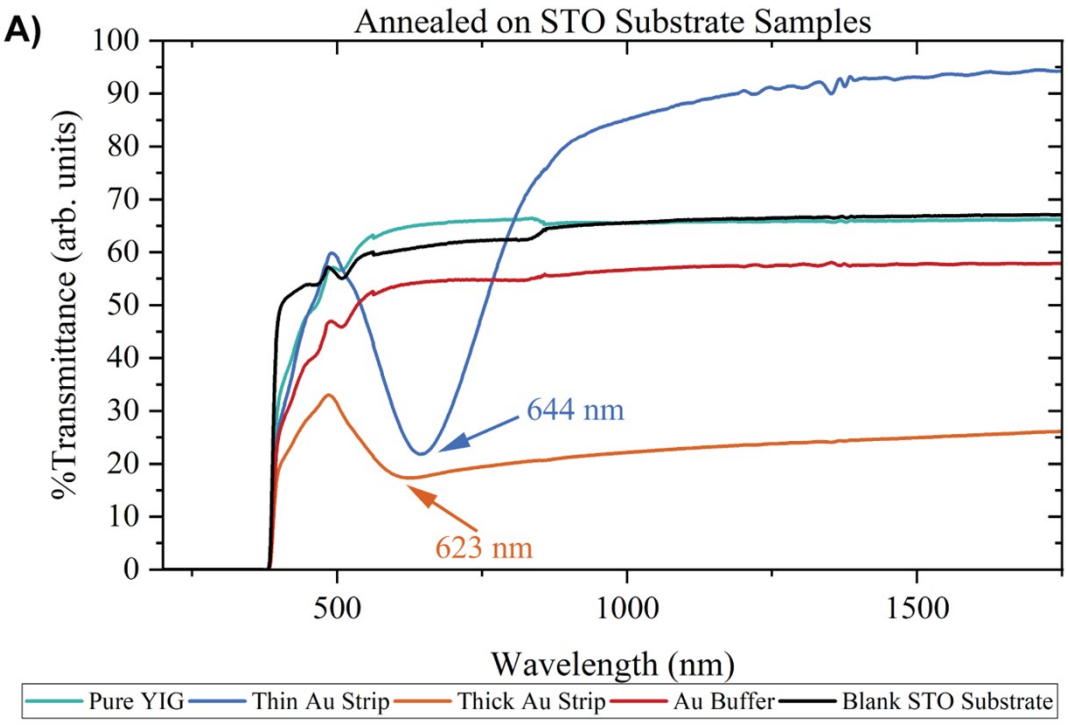

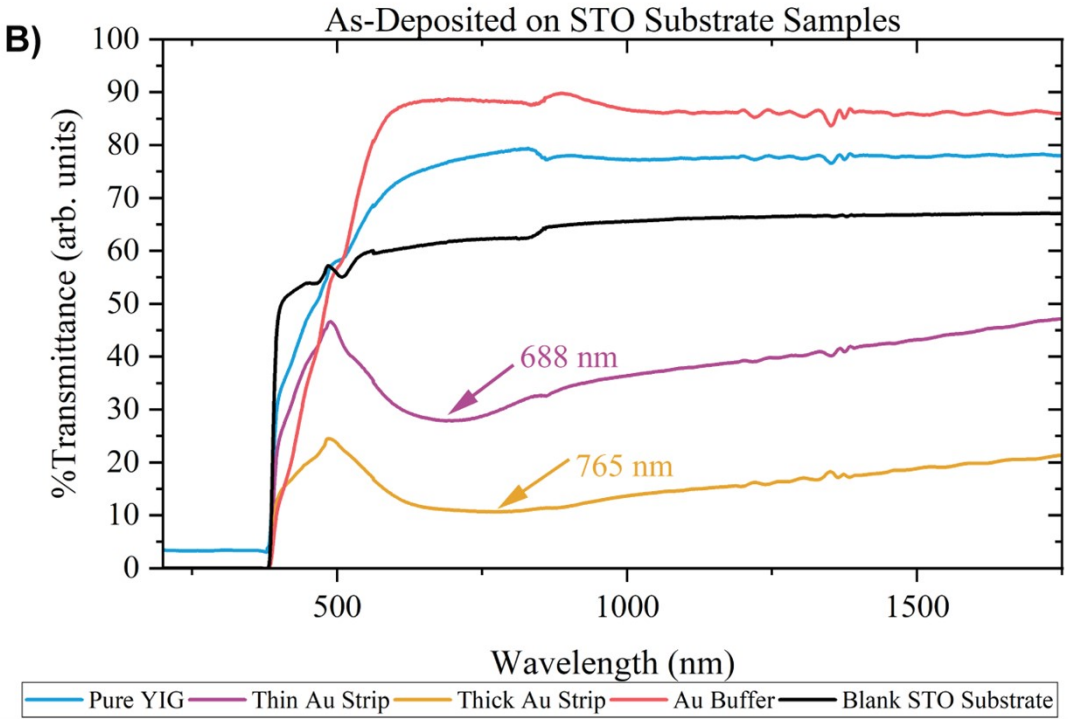

Figure S17: A) Transmittance data for the Annealed samples on STO substrates. B) Transmittance data for the As-Deposited samples on STO substrates. Both have plasmonic resonances marked as needed.

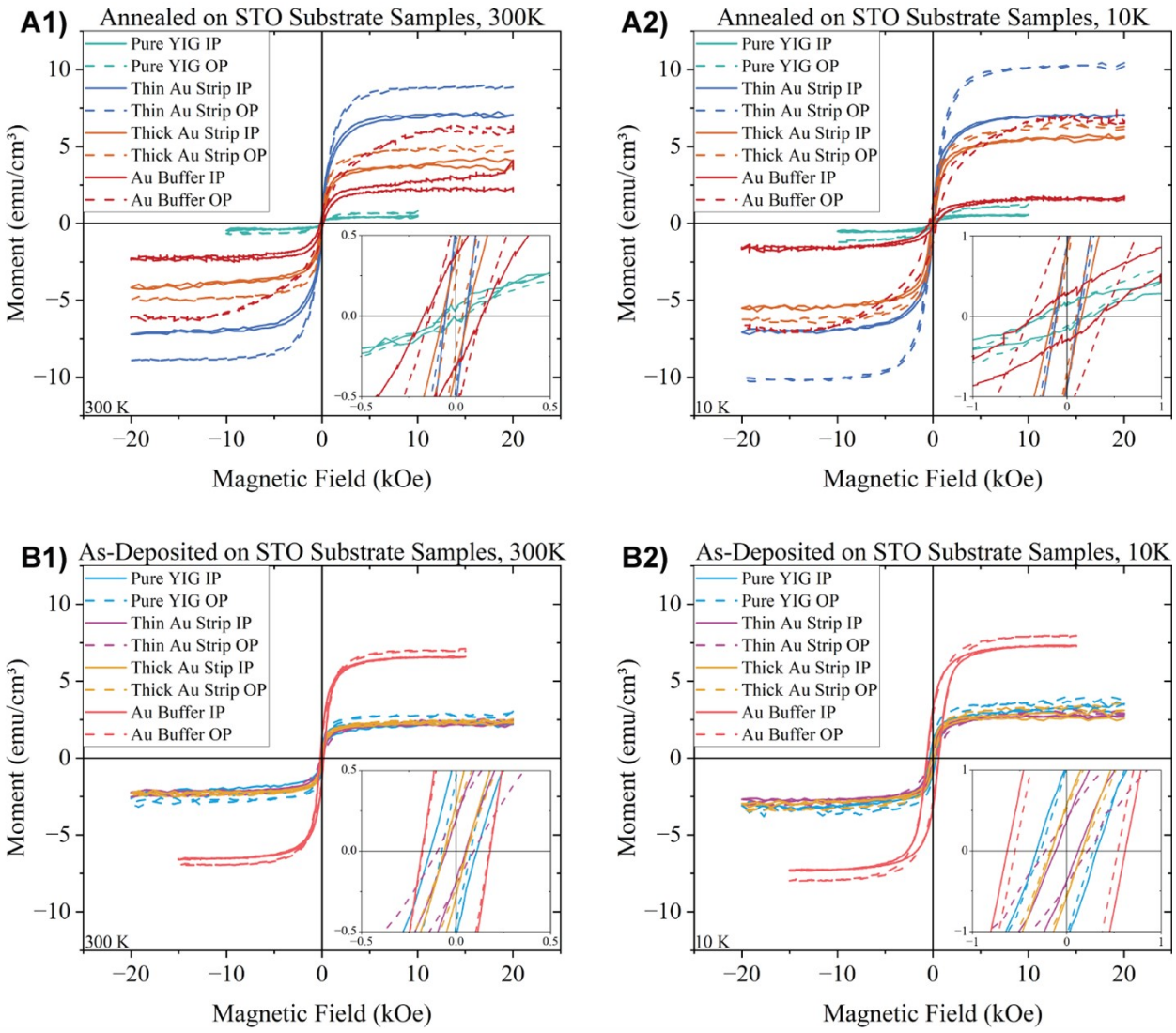

Figure S18: Magnetic hysteresis data for the Annealed samples on STO substrates at A1) 300 K and A2) 10 K. For the As-Deposited samples on STO substrates at B1) 300 K and B2) 10 K.

Table S6: List of the Saturation Magnetization and Coercivity for all the samples grown on STO substrates.

		300 K		10 K	
		Saturation (emu/cm^3)	Coercivity (kOe)	Saturation (emu/cm^3)	Coercivity (kOe)
Annealed Pure YIG	IP	0.42	0.064	0.52	0.272
	OP	0.66	0.054	1.17	0.193
Annealed Thin Au Strip	IP	7.14	0.053	5.63	0.114
	OP	5.66	0.059	8.16	0.133
Annealed Thick Au Strip	IP	3.97	0.067	6.08	0.154
	OP	4.93	0.036	6.33	0.101
Annealed Au Buffer	IP	2.44	0.154	1.62	0.346
	OP	6.05	0.134	6.82	0.402
As-Deposited Pure YIG	IP	2.39	0.060	2.85	0.163
	OP	2.42	0.058	3.31	0.175
As-Deposited Thin Au Strip	IP	2.21	0.051	2.72	0.121
	OP	2.45	0.097	3.03	0.225
As-Deposited Thick Au Strip	IP	2.29	0.060	2.89	0.164
	OP	2.46	0.058	3.34	0.175
As-Deposited Au Buffer	IP	6.58	0.181	7.27	0.626
	OP	6.97	0.176	7.96	0.548

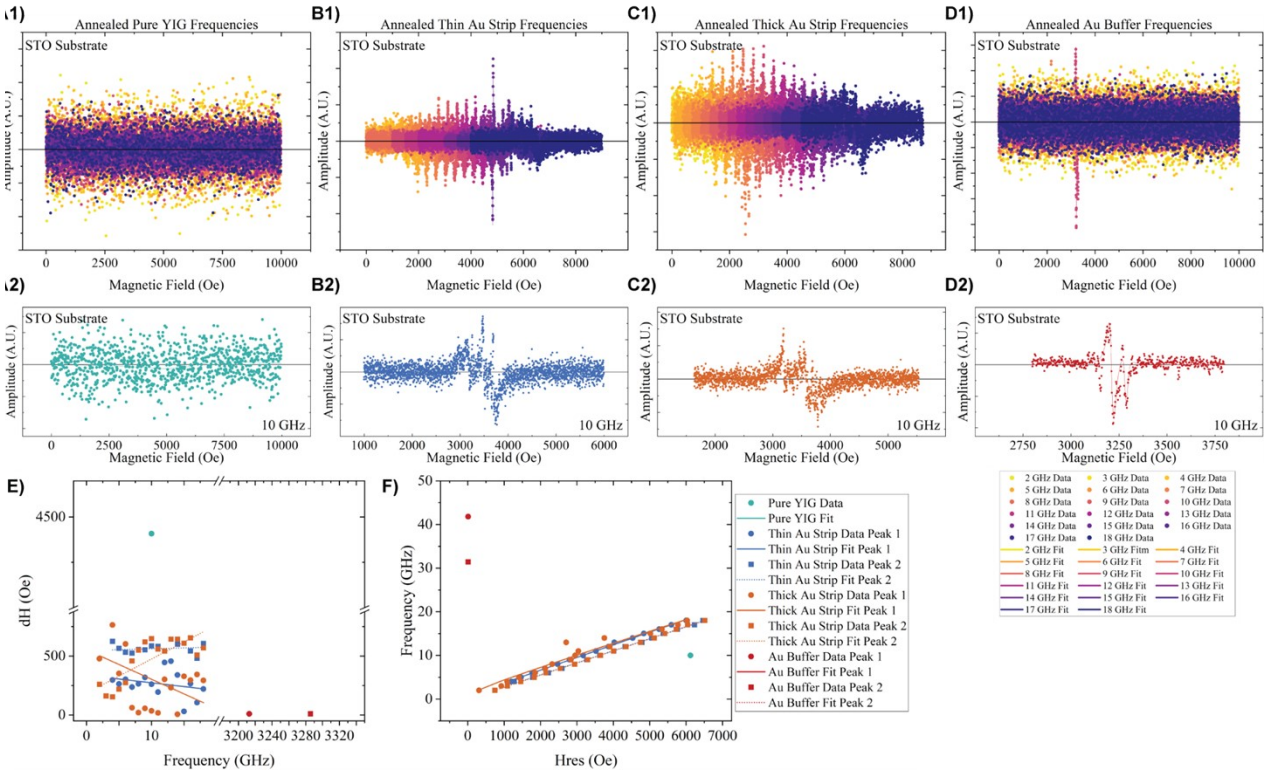

Figure S19: Ferromagnetic resonance measurement results of the Annealed samples on STO substrates A) Pure YIG, B) Thin Au Strip, C) Thick Au Strip, D) Au Buffer. 1) All measured frequencies. 2) Selected 10 GHz frequency. E) Graph showing the width of the frequency peaks versus the frequency they appear at for all four shown samples. F) Graph showing the frequency resonance peaks appear at versus where the peaks occur for all four shown samples.

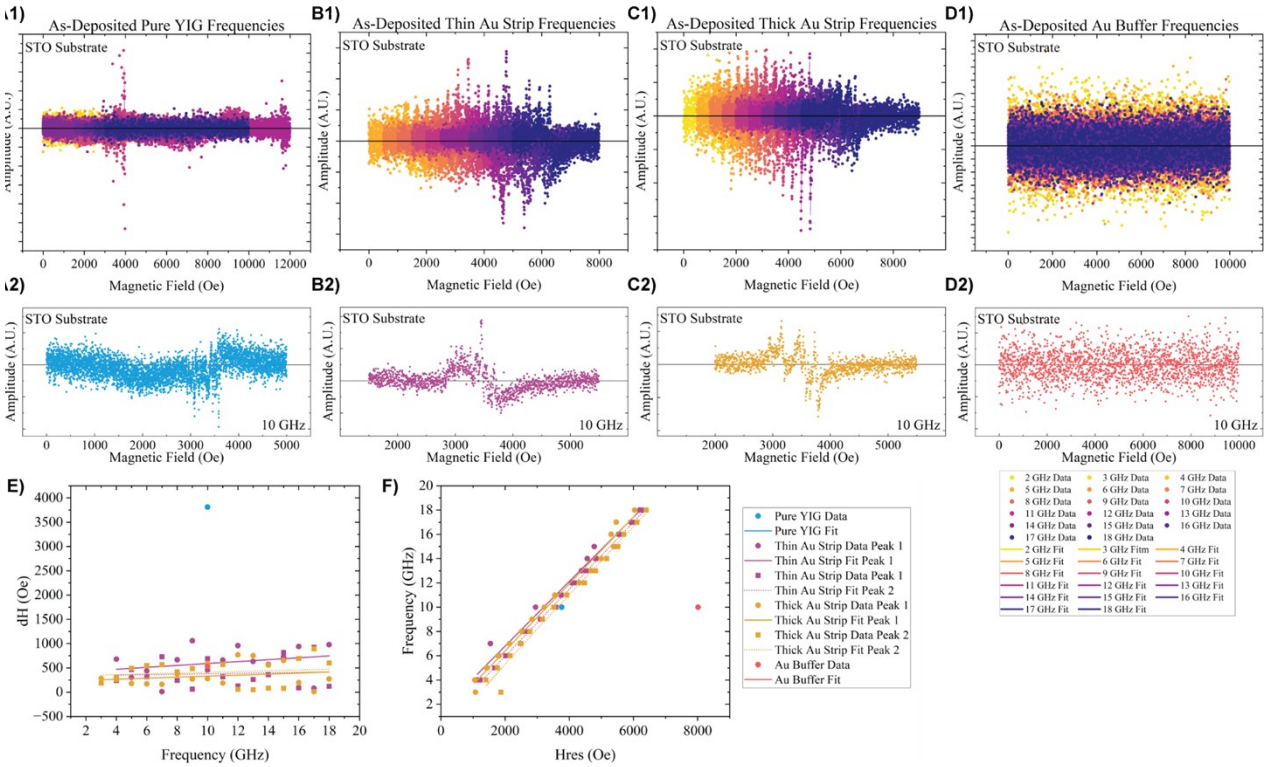

Figure S20: Ferromagnetic resonance measurement results of the As-Deposited samples on STO substrates A) Pure YIG, B) Thin Au Strip, C) Thick Au Strip, D) Au Buffer. 1) All measured frequencies. 2) Selected 10 GHz frequency. E) Graph showing the width of the frequency peaks versus the frequency they appear at for all four shown samples. F) Graph showing the frequency resonance peaks appear at versus where the peaks occur for all four shown samples.

Despite some of the samples on STO giving a measurable ferromagnetic resonance response, the number of peaks seen for the samples, up to six, was actually unfittable by the PhaseFMR program. For each frequency, it would average different peaks together to get its maximum of two fittable peaks, leading to very different 'peaks' at each frequency. Due to this, the fitted 'Gilbert damping coefficient' will not be reported here because we know it was fitted incorrectly. The shown FMR data is to demonstrate that these films can have a measurable FMR and if fitted properly, a magnetic damping. The number of peaks seen is also interesting. This is believed to be due to orthorhombic YIG and its splitting into yttrium-rich and iron-rich areas, as seen in the following TEM images.

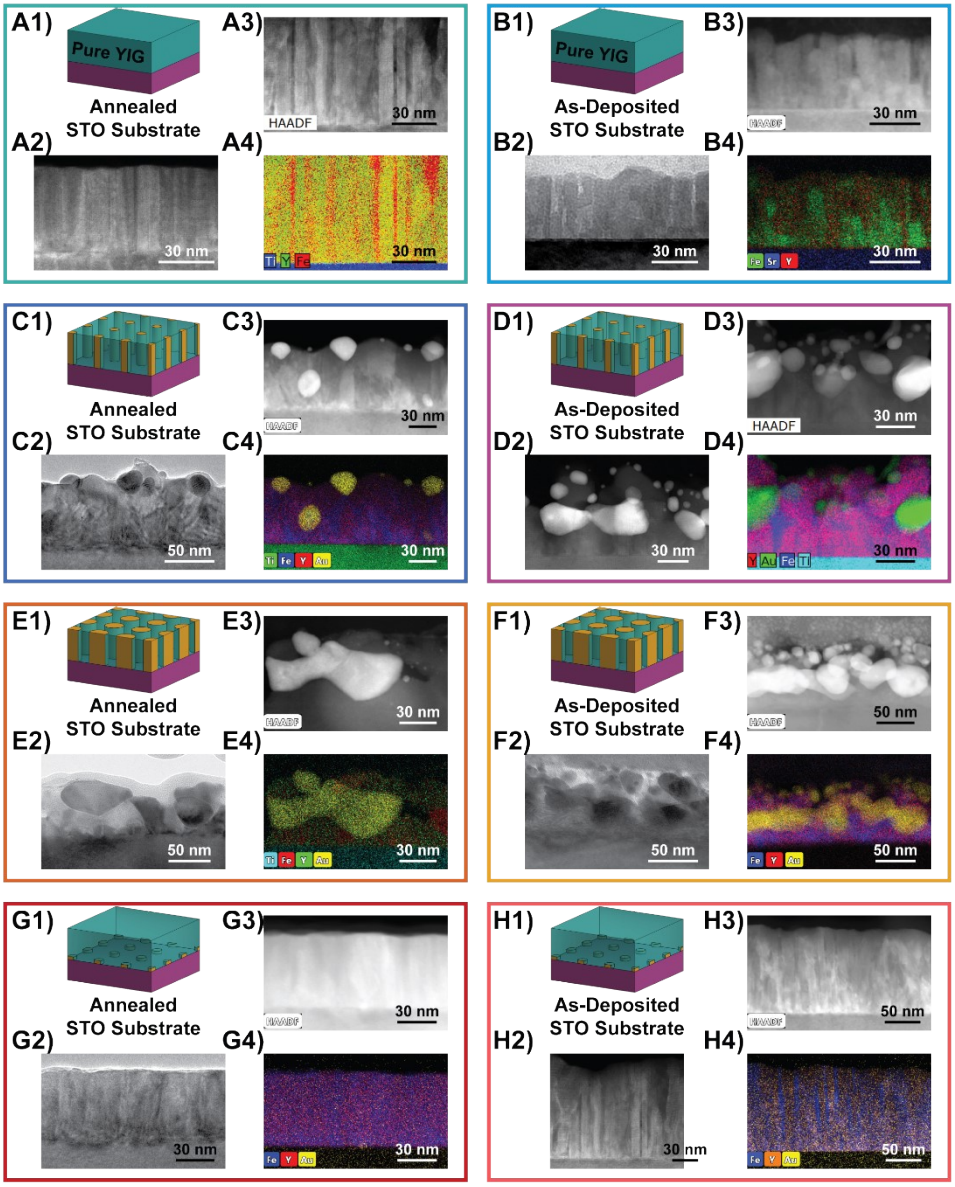

Figure S21: On STO substrates: A) Annealed Pure YIG, B) As-Deposited Pure YIG, C) Annealed Thin Au Strip, D) As-Deposited Thin Au Strip, E) Annealed Thick Au Strip, F) As-Deposited Au Strip, G) Annealed Au Buffer, H) As-Deposited Au Buffer. 1) Ideal schematic drawing of the sample, 2) TEM image of the sample 3) STEM image for the corresponding EDS map of the sample, 4) EDS map of the sample.

Table S7: Sample Thickness of Films grown on STO Substrates

	Film Thickness (nm)
Annealed Pure YIG	51.0
Annealed Thin Au Strip	74.8
Annealed Thick Au Strip	64.8
Annealed Au Buffer	59.3
As-Deposited Pure YIG	45.5
As-Deposited Thin Au Strip	76.9
As-Deposited Thick Au Strip	83.9
As-Deposited Au Buffer	115.9